An Efficient Solution For the Response of Electrical Well Logging Tools in a Complex Environment

Weng Cho Chew, *Senior Member, IEEE,* Zaiping Nie, Qing-Huo Liu, *Member, IEEE,* and Barbara Anderson

***Abstract*—An efficient method for computing the response of some electrical logging tools in a complex environment is presented. This complex environment consists of multiple geological beds with a borehole and invaded zones. The method uses local reflection and transmission operators of a single-bed boundary and a general recursive algorithm to derive generalized reflection and transmission operators. Using this method, the computation time scales linearly as *N*, where *N* is the number of beds in the environment. Hence the method is much more efficient than the finite-element method for solving the same problem. Furthermore, the solution is presented in a symmetric form so that reciprocity can be readily verified.**

I. Introduction

WELL-LOGGING, whereby sensing instruments are lowered into boreholes to measure the physical properties of the subsurface earth, is an important part of geophysical exploration. Among well-logging tools, electrical (or electromagnetic) tools which measure conductivities (or resistivities) and dielectric constants are essential. In oil exploration, for instance, oil-impregnated rocks have a higher resistivity than water-saturated rocks, because connate water is conductive, whereas oil is an insulator. As such, the resistivity of rocks is a good indicator of the presence of hydrocarbon. On the other hand, water has a high dielectric constant of $80\epsilon_0$, which is much greater than that of oil, being about $2\epsilon_0$. Hence the dielectric constant measurement is a good indicator of the presence of water [1].

Electromagnetic well-logging tools are designed to inject or induce current flow in the rock formation. For example, laterologs inject currents into the rock formation by using electrodes. However, the induction tools induce eddy currents in a rock formation using a current loop which generates a time-varying magnetic field. The manner in which the formation responds to the field excited by the source can then be used to determine the resistivity and dielectric constant of the rock formation [2].

In a homogeneous formation a simple formula can usually be derived for the conductivity and dielectric constant. This is measured by a logging tool. Unfortunately, the real environment in which the tool operates consists of complex inhomogeneities. Such complex inhomogeneities can make the interpretation of well-logging measurements extremely difficult. Hence it is often necessary to ascertain how a complex environment confuses the log interpretation process and to refine the interpretation if patterns are observed.

One way to ascertain the effect of a complex environment is to perform experiments. However, experiments are often expensive and physical parameters cannot be altered easily. An alternative is to perform computer modeling. Computer modeling cuts the cost of such studies, because the physical parameters in a model can be altered easily. Moreover, advances in computer technology are rapidly decreasing the cost of such studies.

In this paper we shall discuss the computer modeling of the response of an electromagnetic source in a two-dimensional well-logging environment. The environment consists of a borehole and horizontal beds, with invaded zones in the beds. Moreover, the number of beds is arbitrary. In theory, the field equations can be solved by the finite-element method. However, a routine application of the finite-element method results in the use of an exorbitantly large amount of computer memory, along with lengthy computer run-times. On the other hand, a combined use of numerical and analytic methods can result in a great savings in computational resources. Such a method is known variously as the semi-analytic method or the hybrid method [3]-[10]. We shall call it the numerical mode-matching method due to its resemblance to mode matching [11]-[14]. The method also has a recursive structure, so that its implementation on a computer is straightforward. Moreover, the computation effort grows linearly with the number of beds, rendering it very efficient. This work differs from the work in [10] because here, generalized reflection and transmission operators which are derived recursively are used to propagate the wave through different regions. In [10], a generalized Haskell matrix is used to propagate the wave through different regions. The method described here is more like the geometric optics ray series approach, whereas [10] uses a method more akin to the propagator matrix approach [15].

The numerical mode-matching method reduces a higher-dimensional problem to a lower-dimensional one in which the modes are found numerically. These modes are then propagated through the higher dimension analytically using mode propagators. For example, a two-dimensional problem involving (ρ, z) is reduced to a one-dimensional problem involving only ρ from which the modes are found numerically. These modes are then propagated in the z direction analytically with mode propagators. Hence the modes can propagate through large distances without much computational effort. When a discontinuity is present, the reflection, transmission, and conversion of modes are characterized by reflection and transmission operators. These operators are easily derived for a single-discontinuity problem [3]-[5]. When many discontinuities are present, they can be

Manuscript received May 4, 1990; revised November 1, 1990. This work was supported by the National Science Foundation through Grant NSF ECS-85-25891 and by Schlumberger-Doll Research. The computer time was partially provided by the National Center for Supercomputer Applications at the University of Illinois.

W. C. Chew and Z. Nie are with the Electromagnetics Laboratory, Department of Electrical and Computer Engineering, University of Illinois, Urbana, IL 61801.

Q.-H. Liu and B. Anderson are with Schlumberger-Doll Research, Old Quarry Road, Ridgefield, CT 06877.

IEEE Log Number 9041827.

0196-2892/91/0300-0308$01.00 © 1991 IEEE

treated as a concatenation of one-discontinuity problems [8]. In this manner multiple reflections and transmissions are easily accounted for with generalized reflection and transmission operators using a recursive algorithm.

We will present the result here in a symmetrical form so that reciprocity is readily verified.

II. Theory

First, consider the case where the inhomogeneity is translationally invariant in the z direction (i.e., no z variation in the inhomogeneity). Then the field due to a source can be written as [3]–[5]:

$$\rho A_\phi = \mathbf{f}^t(\rho)\cdot e^{i\overline{\mathbf{k}}_z|z-z'|}\cdot \overline{\mathbf{k}}_z^{-1}\cdot \mathbf{f}(\rho') \tag{1}$$

where $\mathbf{f}(\rho)$ is a column vector containing $f_i(\rho)$, the ith eigenvector; $\overline{\mathbf{k}}_z$ is a diagonal matrix containing k_{iz} on the diagonal; and ρ' and z' are source coordinates. Hence $e^{i\overline{\mathbf{k}}_z|z-z'|}$ is a propagator that propagates the modes through a distance $|z-z'|$. Here, A_ϕ is either E_ϕ or H_ϕ depending on whether we are considering the TE or the TM problem.

Now, if the source is embedded between two bed boundaries, then the field that emanates from the source will be reflected by the bed boundaries. Consequently, (1) has to be augmented by the reflected field terms, consisting of upgoing and downgoing waves. Assuming the source to be in the mth bed region as shown in Fig. 1, then

$$\begin{aligned}\rho A_{m\phi} = \mathbf{f}_m^t(\rho)\cdot\big[e^{i\overline{\mathbf{k}}_{mz}|z-z'|} + e^{i\overline{\mathbf{k}}_{mz}z}\cdot\overline{\mathbf{C}}_m + e^{-i\overline{\mathbf{k}}_{mz}z}\cdot\overline{\mathbf{D}}_m\big]\\ \cdot\,\overline{\mathbf{k}}_{mz}^{-1}\cdot \mathbf{f}_m(\rho').\end{aligned}\tag{2}$$

Here $\overline{\mathbf{C}}_m$ and $\overline{\mathbf{D}}_m$ are unknown matrices yet to be determined. They can be found easily if the generalized reflection operators of the beds above and below the source are known. With these reflection operators, constraint conditions can be written at $z = d_{m-1}$ and $z = d_m$. With the constraint conditions, $\overline{\mathbf{C}}_m$ and $\overline{\mathbf{D}}_m$ can then be found [8].

The constraint conditions at $z = d_{m-1}$ is that the downgoing wave is a consequence of the reflection of the upgoing waves. Assuming the generalized reflection operator here to be $\overline{\overline{\mathbf{R}}}_{m,m-1}$ [8], then it follows that

$$\begin{aligned}&e^{-i\overline{\mathbf{k}}_{mz}d_{m-1}}\cdot\overline{\mathbf{D}}_m\\ &\quad = \overline{\overline{\mathbf{R}}}_{m,m-1}\cdot\big(e^{i\overline{\mathbf{k}}_{mz}d_{m-1}}\cdot\overline{\mathbf{C}}_m + e^{i\overline{\mathbf{k}}_{mz}|d_{m-1}-z'|}\big).\end{aligned}\tag{3}$$

Applying a similar constraint condition at $z = d_m$ and assuming the reflection operator here to be $\overline{\overline{\mathbf{R}}}_{m,m+1}$, then

$$e^{i\overline{\mathbf{k}}_{mz}d_m}\cdot\overline{\mathbf{C}}_m = \overline{\overline{\mathbf{R}}}_{m,m+1}\cdot\big(e^{-i\overline{\mathbf{k}}_{mz}d_m}\cdot\overline{\mathbf{D}}_m + e^{i\overline{\mathbf{k}}_{mz}|d_m-z'|}\big).\tag{4}$$

Equations (3) and (4) can be solved to yield $\overline{\mathbf{C}}_m$ and $\overline{\mathbf{D}}_m$, which are

$$\begin{aligned}e^{i\overline{\mathbf{k}}_{mz}d_m}\cdot\overline{\mathbf{C}}_m = \overline{\mathbf{M}}_{m+}\cdot\overline{\overline{\mathbf{R}}}_{m,m+1}\cdot\big[e^{i\overline{\mathbf{k}}_{mz}t_m}\cdot\overline{\overline{\mathbf{R}}}_{m,m-1}\\ \cdot\, e^{i\overline{\mathbf{k}}_{mz}|d_{m-1}-z'|} + e^{i\overline{\mathbf{k}}_{mz}|d_m-z'|}\big]\end{aligned}\tag{5}$$

$$\begin{aligned}e^{-i\overline{\mathbf{k}}_{mz}d_{m-1}}\cdot\overline{\mathbf{D}}_m = \overline{\mathbf{M}}_{m-}\cdot\overline{\overline{\mathbf{R}}}_{m,m-1}\cdot\big[e^{i\overline{\mathbf{k}}_{mz}t_m}\cdot\overline{\overline{\mathbf{R}}}_{m,m+1}\\ \cdot\, e^{i\overline{\mathbf{k}}_{mz}|d_m-z'|} + e^{i\overline{\mathbf{k}}_{mz}|d_{m-1}-z'|}\big]\end{aligned}\tag{6}$$

where

$$\overline{\mathbf{M}}_{m+} = \big(\overline{\mathbf{I}} - \overline{\overline{\mathbf{R}}}_{m,m+1}\cdot e^{i\overline{\mathbf{k}}_{mz}t_m}\cdot\overline{\overline{\mathbf{R}}}_{m,m-1}\cdot e^{i\overline{\mathbf{k}}_{mz}t_m}\big)^{-1}\tag{7a}$$

$$\overline{\mathbf{M}}_{m-} = \big(\overline{\mathbf{I}} - \overline{\overline{\mathbf{R}}}_{m,m-1}\cdot e^{i\overline{\mathbf{k}}_{mz}t_m}\cdot\overline{\overline{\mathbf{R}}}_{m,m+1}\cdot e^{i\overline{\mathbf{k}}_{mz}t_m}\big)^{-1}\tag{7b}$$

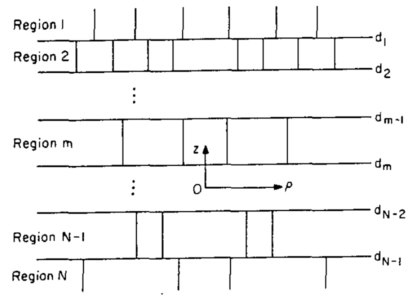

Fig. 1. Geometry of the problem.

and t_m is the thickness of the mth region. Consequently, (5) and (6) can be used in (2) to find the field in region m. The resultant expression after some algebraic manipulations could further be simplified to:

$$\rho A_{m\phi} = \begin{cases} \mathbf{f}_m^t(\rho)\cdot\big[e^{i\overline{\mathbf{k}}_{mz}(z-d_{m-1})} + e^{-i\overline{\mathbf{k}}_{mz}(z-d_{m-1})}\cdot\overline{\overline{\mathbf{R}}}_{m,m-1}\big] \\ \quad\cdot\, e^{i\overline{\mathbf{k}}_{mz}t_m}\cdot\overline{\mathbf{M}}_{m+}\cdot\big[e^{-i\overline{\mathbf{k}}_{mz}(z'-d_m)} \\ \quad + \overline{\overline{\mathbf{R}}}_{m,m+1}\cdot e^{i\overline{\mathbf{k}}_{mz}(z'-d_m)}\big]\cdot\overline{\mathbf{k}}_{mz}^{-1}\cdot \mathbf{f}_m(\rho'), \\ \quad z > z' \\ \mathbf{f}_m^t(\rho)\cdot\big[e^{-i\overline{\mathbf{k}}_{mz}(z-d_m)} + e^{i\overline{\mathbf{k}}_{mz}(z-d_m)}\cdot\overline{\overline{\mathbf{R}}}_{m,m+1}\big] \\ \quad\cdot\, e^{i\overline{\mathbf{k}}_{mz}t_m}\cdot\overline{\mathbf{M}}_{m-}\cdot\big[e^{i\overline{\mathbf{k}}_{mz}(z'-d_{m-1})} \\ \quad + \overline{\overline{\mathbf{R}}}_{m,m-1}\cdot e^{-i\overline{\mathbf{k}}_{mz}(z'-d_{m-1})}\big]\cdot\overline{\mathbf{k}}_{mz}^{-1}\cdot \mathbf{f}_m(\rho'), \\ \quad z < z'. \end{cases}\tag{8}$$

As the manipulation that leads to (8) from (2) is rather complex, the interested reader is encouraged to first work with a scalar version of both (2) and (8). After having obtained the insight of the algebraic manipulation for the scalar case, that the vector case can be gotten similarly except now, the orders of the operators are important.

The preceding expression has the advantage of being symmetrical between the source point and observation point. Hence the reciprocity theorem is readily verified from it [5].

Now if the observation point is in region n, where $n < m$ but the source is still in region m, the field can then be written as

$$\begin{aligned}\rho A_{n\phi} = \mathbf{f}_n^t(\rho)\cdot\big[e^{i\overline{\mathbf{k}}_{nz}z} + e^{-i\overline{\mathbf{k}}_{nz}(z-d_{n-1})}\\ \cdot\,\overline{\overline{\mathbf{R}}}_{n,n-1}\cdot e^{i\overline{\mathbf{k}}_{nz}d_{n-1}}\big]\cdot\mathbf{A}_n.\end{aligned}\tag{9}$$

Here $\mathbf{A}_n$ is a vector denoting the amplitude of the upgoing wave in region n. It can be related to the amplitude of the upgoing wave in region m as [8]

$$\begin{aligned}e^{i\overline{\mathbf{k}}_{nz}d_n}\cdot\mathbf{A}_n &= \overline{\mathbf{D}}_{n+}\cdot\overline{\mathbf{T}}_{n+1,n}\cdot e^{i\overline{\mathbf{k}}_{n+1,z}t_{n+1}}\cdot\overline{\mathbf{D}}_{n+1,+}\cdot\overline{\mathbf{T}}_{n+2,n+1}\\ &\quad\cdot\, e^{i\overline{\mathbf{k}}_{n+2,z}t_{n+2}}\cdot\overline{\mathbf{D}}_{n+3,+}\cdot\overline{\mathbf{T}}_{n+3,n+2}\\ &\quad\cdot\, e^{i\overline{\mathbf{k}}_{n+3,z}t_{n+3}}\cdots e^{i\overline{\mathbf{k}}_{m-1,z}t_{m-1}}\cdot\overline{\mathbf{D}}_{m-1,+}\\ &\quad\cdot\,\overline{\mathbf{T}}_{m,m-1}\cdot e^{i\overline{\mathbf{k}}_{mz}d_{m-1}}\cdot\mathbf{A}_m\\ &= \left(\prod_{i=n}^{m-2}\overline{\mathbf{D}}_{i+}\cdot\overline{\mathbf{T}}_{i+1,i}\cdot e^{i\overline{\mathbf{k}}_{i+1,z}t_{i+1}}\right)\cdot\overline{\mathbf{D}}_{m-1,+}\\ &\quad\cdot\,\overline{\mathbf{T}}_{m,m-1}\cdot e^{i\overline{\mathbf{k}}_{mz}d_{m-1}}\cdot\mathbf{A}_m\end{aligned}\tag{10}$$

where

$$\overline{D}_{i+} = (\overline{I} - \overline{R}_{i,i+1} \cdot e^{i\overline{k}_{iz}t_i} \cdot \overline{\overline{R}}_{i,i-1} \cdot e^{i\overline{k}_{iz}t_i})^{-1} \qquad (11)$$

and $\overline{T}_{ij}$ is a local transmission operator at a bed boundary. The order of the operator is important in (10). Using (10), a generalized transmission operator between region m and n can be defined such that

$$e^{i\overline{k}_{nz}d_n} \cdot A_n = \overline{\overline{T}}_{mn} \cdot e^{i\overline{k}_{mz}d_{m-1}} \cdot A_m. \qquad (12)$$

It relates the upgoing wave amplitude at $z = d_{m-1}$ to the upgoing wave amplitude at $z = d_n$. On comparing (10) and (12), the definition of $\overline{\overline{T}}_{mn}$ can be deduced.

From (8) we notice that the upgoing wave amplitude at $z = d_{m-1}$ is

$$e^{i\overline{k}_{mz}d_{m-1}} \cdot A_m = e^{i\overline{k}_{mz}t_m} \cdot \overline{M}_{m+} \cdot [e^{-i\overline{k}_{mz}(z'-d_m)} + \overline{\overline{R}}_{m,m+1} \cdot e^{i\overline{k}_{mz}(z'-d_m)}] \cdot \overline{k}_{mz}^{-1} \cdot f_m(\rho'). \qquad (13)$$

Consequently, (9) becomes:

$$\rho A_{n\phi} = f_n^t(\rho) \cdot [e^{i\overline{k}_{nz}(z-d_{n-1})} + e^{-i\overline{k}_{nz}(z-d_{n-1})} \cdot \overline{\overline{R}}_{n,n-1}] \cdot e^{i\overline{k}_{nz}t_n} \cdot \overline{\overline{T}}_{mn} \cdot e^{i\overline{k}_{mz}t_m} \cdot \overline{M}_{m+} \cdot [e^{-i\overline{k}_{mz}(z'-d_m)} + \overline{\overline{R}}_{m,m+1} \cdot e^{i\overline{k}_{mz}(z'-d_m)}] \cdot \overline{k}_{mz}^{-1} \cdot f_m(\rho'). \qquad (14)$$

The above form is symmetrical between the source point and observation point so that reciprocity can be readily proven.

Similarly, if the observation point is in region l, where $l > m$, the field in region l can be written as

$$\rho A_{l\phi} = f_l^t(\rho) \cdot [e^{-i\overline{k}_{lz}z} + e^{i\overline{k}_{lz}(z-d_l)} \cdot \overline{\overline{R}}_{l,l+1} \cdot e^{-i\overline{k}_{lz}d_l}] \cdot B_l. \qquad (15)$$

Here B_l is a vector denoting the amplitude of the downgoing wave in region l. It can be related to the amplitude of the downgoing wave in region m as

$$\begin{aligned} e^{-i\overline{k}_{lz}d_{l-1}} \cdot B_l &= \overline{D}_{l-} \cdot \overline{T}_{l-1,l} \cdot e^{i\overline{k}_{l-1,z}t_{l-1}} \cdot \overline{D}_{l-1,-} \cdot \overline{T}_{l-2,l-1} \\ &\quad \cdot e^{i\overline{k}_{l-2,z}t_{l-2}} \cdots e^{i\overline{k}_{m+1,z}t_{m+1}} \cdot \overline{D}_{m+1,+} \\ &\quad \cdot \overline{T}_{m,m+1} \cdot e^{i\overline{k}_{mz}d_{m+1}} \cdot B_m \\ &= \left(\prod_{i=l}^{m+2} \overline{D}_{i+} \cdot \overline{T}_{i-1,i} \cdot e^{i\overline{k}_{i-1,z}t_{i-1}} \right) \cdot \overline{D}_{m+1,+} \\ &\quad \cdot \overline{T}_{m,m+1} \cdot e^{i\overline{k}_{mz}d_{m+1}} \cdot B_m \end{aligned} \qquad (16)$$

where

$$\overline{D}_{i+} = (\overline{I} - \overline{R}_{i,i-1} \cdot e^{i\overline{k}_{iz}t_i} \cdot \overline{\overline{R}}_{i,i+1} \cdot e^{i\overline{k}_{iz}t_i})^{-1} \qquad (17)$$

and $\overline{T}_{ij}$ is a local transmission operator at a bed boundary. The order of operators is important in (16). With (16), a generalized transmission operator between region m and l can be defined such that

$$e^{-i\overline{k}_{lz}d_{l-1}} \cdot B_l = \overline{\overline{T}}_{ml} \cdot e^{-i\overline{k}_{mz}d_m} \cdot B_m. \qquad (18)$$

It relates the downgoing wave amplitude at $z = d_m$ to the downgoing wave amplitude at $z = d_{l-1}$. The definition of $\overline{\overline{T}}_{ml}$ can be deduced on comparing (16) and (18).

From (18), we notice that the downgoing wave amplitude at $z = d_m$ is

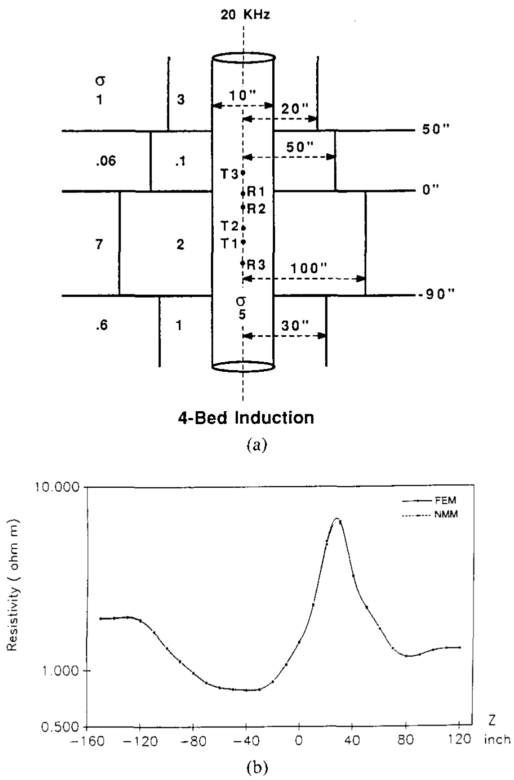

Fig. 2. (a) Parameters of a four-bed geometry modeled at 20 KHz for the 6FF40 induction tool with three transmitters and three receivers. (b) Comparison between the numerical mode-matching method and the finite-element method for the geometry shown in (a).

$$e^{-i\overline{k}_{mz}d_m} \cdot B_m = e^{i\overline{k}_{mz}t_m} \cdot \overline{M}_{m-} \cdot [e^{i\overline{k}_{mz}(z'-d_{m-1})} + \overline{\overline{R}}_{m,m-1} \cdot e^{-i\overline{k}_{mz}(z'-d_{m-1})}] \cdot \overline{k}_{mz}^{-1} \cdot f_m(\rho'). \qquad (19)$$

Consequently, (15) becomes:

$$\rho A_{l\phi} = f_l^t(\rho) \cdot [e^{-i\overline{k}_{lz}(z-d_l)} + e^{i\overline{k}_{lz}(z-d_l)} \cdot \overline{\overline{R}}_{l,l+1}] \cdot e^{i\overline{k}_{lz}t_l} \cdot \overline{\overline{T}}_{ml} \cdot e^{i\overline{k}_{mz}t_m} \cdot \overline{M}_{m-} \cdot [e^{-i\overline{k}_{mz}(z'-d_m)} + \overline{\overline{R}}_{m,m+1} \cdot e^{i\overline{k}_{mz}(z'-d_m)}] \cdot \overline{k}_{mz}^{-1} \cdot f_m(\rho'). \qquad (20)$$

This form is symmetrical between the source point and observation point so that reciprocity is easily proven.

III. Results

A computer program has been developed that executes the above formulation. Results have been compared with results from the finite-element method. Comparisons with the two-dimensional finite-element method [16] have been made at 20 KHz, the frequency of the induction tool, as well as at 25 MHz, the frequency of the deep propagation tool (DPT) [17], [18]. Excellent agreement has been noted between the results of the numerical mode-matching method described above and the finite-element method. However, the numerical mode-matching code is much faster than the general finite-element code. The increase in speed is a consequence of treating the problem an-

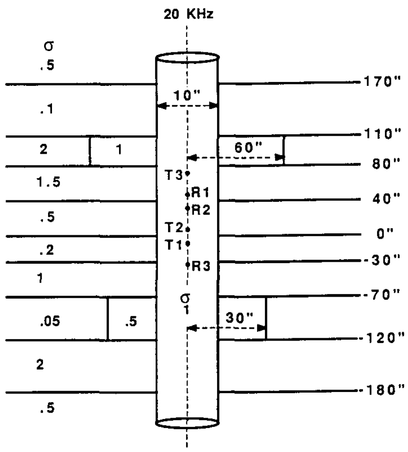

10-Bed Induction

(a)

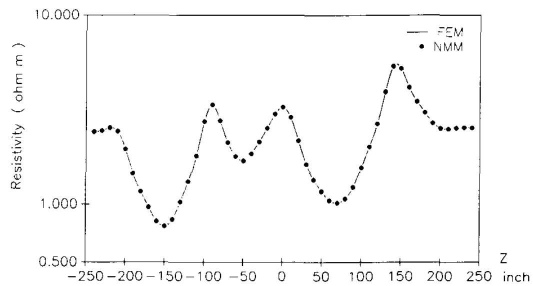

(b)

Fig. 3. (a) A ten-bed geometry for induction logging. (b) Comparison between the numerical mode-matching method and the finite-element method for the geometry shown in (a).

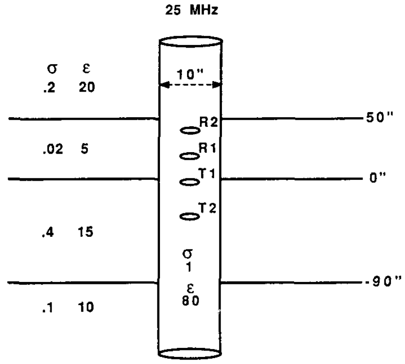

4-Bed DPT

(a)

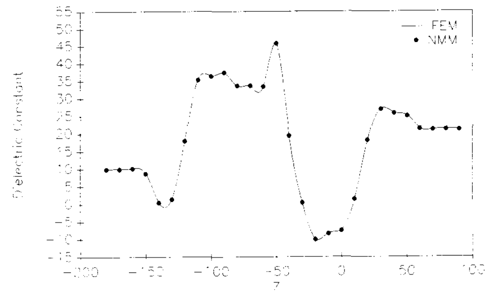

(b)

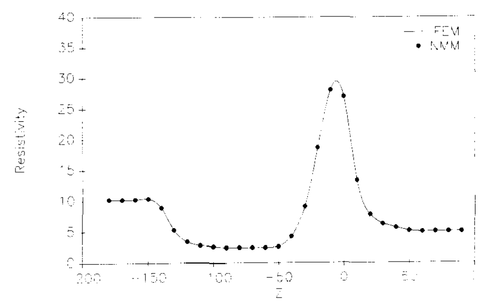

(c)

Fig. 4. (a) A four-bed geometry for the DPT at 25 MHz. (b) Comparison between the numerical mode-matching method and the finite-element method for the apparent dielectric constant for the geometry shown in (a). (c) Comparison between the numerical mode-matching method and the finite-element method for the apparent resistivity for the same case.

alytically in the z direction, while solving the problem in the ρ direction numerically as only a one-dimensional finite-element method [3]–[5].

Shown in Fig. 2(a) is a four-bed geometry for modeling the induction tool response, with one invaded zone in each layer. The conductivities and dimensions of the layers are shown in the figure, along with the induction tool. The tool is the 6FF40, with three transmitters and three receivers operating at 20 KHz. Shown in Fig. 2(b) is a comparison of the apparent resistivity obtained by the numerical mode-matching method (NMM) and finite-element method (FEM). Excellent agreement is observed.

Fig. 3(a) shows a ten-bed geometry for induction logging in the invaded zone in layers 3 and 8, respectively. The comparison of the computed apparent resistivity obtained by NMM and FEM in Fig. 3(b) shows very good agreement between these two methods.

The NMM is also used to model DPT response in complicated borehole environments. The DPT operates at 25 MHz, which is much higher than the induction tool frequency. Fig. 4(a) shows a four-bed geometry for modeling the DPT response. There is no borehole fluid invasion present. Fig. 4(b) shows the apparent dielectric constant calculated by NMM for DPT, along with the result obtained by FEM. Fig. 4(c) shows the corresponding apparent resistivity. The agreement between NMM and FEM is excellent in both cases.

Fig. 5(a) illustrates a ten-bed geometry for modeling the DPT response. There is one invaded zone in layers 2 and 8, respectively. The dielectric constants and conductivities of the various regions are shown in the figure. Fig. 5(b) and (c) shows a comparison of the apparent dielectric constant and apparent resistivity, respectively, obtained by the NMM and FEM. Again, the agreement between the two methods is very good. However, the numerical mode-matching method is far more efficient than the finite-element method. For this particular ten-bed geometry, the computation time for the NMM is about 8.6 s, while it is about 630 s for the FEM, when the codes were run on a Cray X-MP/14. Hence the NMM is about 73 times faster than the FEM. In addition, the NMM requires less computer memory than the FEM. This makes the NMM simulation possible even

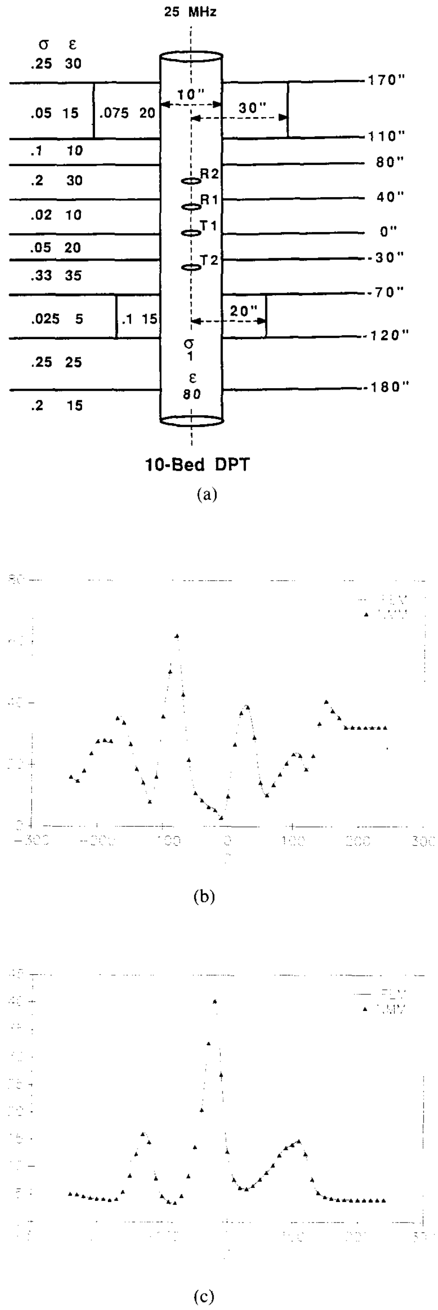

Fig. 5. (a) A ten-bed geometry for the DPT at 25 MHz. (b) Comparison between the numerical mode-matching method and the finite-element method for the apparent dielectric constant for the geometry in (a). (c) Comparison for the apparent resistivity for the same case.

on a small computer such as a VAX, where the FEM code takes hours to generate results. The long FEM computer run-time on a virtual memory machine such as a VAX is a result of the large number of page-faults. The ten-bed NMM case takes about 248 s on a VAX, which is still faster than the FEM code running on the CRAY.

IV. Conclusions

A symmetrical form of the solution for an electrical source in a multibed well logging environment has been derived. The symmetric solution readily renders the proof of reciprocity. A computer program has been developed to implement the solution. The program is robust and generates accurate results from 20 KHz to 25 MHz, achieving excellent agreement with the finite-element method solution of the same problem. However, the method discussed here is many times more efficient than the finite-element method. This efficient method has important applications in the computer-aided design of well-logging tools, as well as in the computer-aided interpretation of well logs.

References

[1] P. N. Sen and W. C. Chew, "The frequency-dependent dielectric and conductivity response of sedimentary rocks," *J. Microwave Power*, vol. 18, no. 1, p. 95, 1983.

[2] D. V. Ellis, *Well Logging for Earth Scientists.* New York: Elsevier, 1987.

[3] W. C. Chew, S. Barone, and C. H. Hennessy, "Diffraction of waves by discontinuities in open, cylindrical structures," in *1983 Int. Symp. Dig., Antennas Propagat.*, May 23-26, 1983, vol. 2, p. 503.

[4] B. Anderson and W. C. Chew, "A new high speed technique for calculating synthetic induction and DPT logs," presented at the SPWLA 25th Ann. Logging Symp., June 1984, paper HH.

[5] W. C. Chew, S. Barone, C. Hennessy, and B. Anderson, "Diffraction of axisymmetric waves in a borehole by bed boundary discontinuities," *Geophysics*, vol. 49, no. 10, p. 1586, Oct. 1984.

[6] L. Tsang, A. K. Chan, and S. Gianzero, "Solution of the fundamental problem in resistivity logging with a hybrid method," *Geophysics*, vol. 49, no. 10, p. 1596, 1984.

[7] B. Anderson and W. C. Chew, "SFL interpretation using high speed synthetic computer generated logs," presented at the SPWLA 26th Ann. Logging Symp., June 1985.

[8] W. C. Chew and B. Anderson, "Propagation of electromagnetic waves through geological beds in a geophysical probing environment," *Radio Sci.*, vol. 20, no. 3, pp. 611-621, May-June 1985.

[9] B. Anderson and W. C. Chew, "A general semi-analytic method for the rapid computer simulation of the response of borehole electrical logging tools," presented at the SEG 55th Int. Meet., Oct. 1985.

[10] D. M. Pai and M. Huang, "A generalized Haskell matrix method for borehole electromagnetics: Theory and applications," *Geophysics*, vol. 53, no. 12, pp. 1577-1586, 1988.

[11] W. C. Chew, "Modeling of the high frequency dielectric logging tool: Theory," *IEEE Trans. Geosci. Remote Sensing*, vol. 26, p. 382, July 1988.

[12] W. C. Chew, "Modeling of the high frequency dielectric logging tool: Applications and results," *IEEE Trans. Geosci. Remote Sensing*, vol. 26, p. 388, July 1988.

[13] Q. Liu and W. C. Chew, "Numerical mode-matching method for the multiregion, vertically stratified media," *IEEE Trans. Antennas Propagat.*, vol. 38, pp. 498-506, 1990.

[14] Q. H. Liu, W. C. Chew, M. R. Taherian, and K. A. Safinya, "A modeling study of electromagnetic propagation tool in complicated borehole environments," *Log Analyst*, vol. 30, no. 6, Nov.-Dec. 1989.

[15] W. C. Chew, *Waves and Fields in Inhomogeneous Media.* New York: Van Nostrand Reinhold, 1990.

[16] B. Anderson and S. K. Chang, "Synthetic induction logs by the finite element method," *Log Analyst*, vol. 23, no. 6, pp. 17-26, 1982.

[17] G. Huchital, "Apparatus and method for determination of subsurface permittivity and conductivity," U.S. Patent No. 4 209 747, June 24, 1980.

[18] G. Huchital, R. Hutin, Y. Thoraval, and B. Clark, "The deep propagation tool," presented at the SPE AIME Meet., Sept. 1982, Paper SPE 10988.

Weng Cho Chew (S'79–M'80–SM'86) was born on June 9, 1953 in Malaysia. He received the B.S. degree in 1976, both the M.S. and engineer's degrees in 1978, and the Ph.D. degree in 1980, all in electrical engineering from the Massachusetts Institute of Technology, Cambridge.

His research interest has been in the area of wave propagation and interaction with heterogeneous media for geophysical subsurface sensing, microwave and millimeter wave applications, mixed boundary value problems for microwave integrated circuits, and microstrip antenna applications. He has also studied electromechanical and dielectric properties of rocks. From 1981 to 1985 he was with Schlumberger-Doll Research, Ridgefield, CT. While he was there he had been a Program Leader and a Department Manager. Currently, he is a Professor with the Department of Electrical and Computer Engineering, University of Illinois at Urbana-Champaign.

Qing-Huo Liu (S'88–M'89) was born in Fujian, China, on February 4, 1963. He received the B.S. and M.S. degrees, both in physics, from Xiamen University, China, in 1983 and 1986, respectively, and the Ph.D. degree in electrical engineering from the University of Illinois, Urbana, in 1989.

His research interest has been in electron paramagnetic resonance spectroscopy, experiments and simulation of transient electron paramagnetic resonance, microstrip antenna applications, electromagnetic wave propagation in inhomogeneous media and optical fibers, geophysical subsurface sensing, and transient electromagnetics. From September 1986 to December 1988 he was a Research Assistant in the Electromagnetics Laboratory at the University of Illinois, Urbana. From January 1989 to February 1990 he was a Postdoctoral Research Associate at the same laboratory. He is currently a Research Scientist with Schlumberger-Doll Research, Ridgefield, CT.

Dr. Liu is a member of Phi Kappa Phi and Tau Beta Pi.

Zaiping Nie was born in Xi'an, China, on October 2, 1946. He graduated from the Chengdu Institute of Radio Engineering (CIRE), Chengdu, in 1968, where he also received the M.S. degree in electromagnetic engineering in 1981.

Since then he has been with CIRE, where he has worked on modified Cassegrain antenna, time-domain antenna, and some scattering problems. He has held the position of Associate Professor since 1987. From 1988 to 1989 he was a Visiting Scholar with the Electromagnetic Laboratory, University of Illinois at Urbana-Champaign. His research interests include electromagnetic scattering theory, microstrip antenna, and wave propagation in inhomogeneous media.

Barbara Anderson obtained the B.S. degree from Western Connecticut State University and did graduate work in mathematics and computer science at Fairfield University (Connecticut).

Since joining Schlumberger-Doll Research, Ridgefield, CT, in 1966, she has developed computer software for use in resistivity tool design and interpretation.

Ms. Anderson is a member of SPE, SPWLA, and SIAM. She received the 1981 SPWLA Symposium Best Paper Award, and "The Log Analyst" Best Paper Awards in 1987 and 1989.